OPTIMIZATION-BASED CALIBRATION OF SOYBEAN SEED DISCRETE ELEMENT PARAMETERS VIA RSM AND GA-BP-GA
/
基于 RSM 和 GA-BP-GA 优化大豆种子仿真参数标定

Shuangcheng XIE, Wensheng YUAN*, Chengqian JIN, Yugang FENG, Fuqiang GOU, Yuqing MA
Nanjing Research Institute for Agricultural Mechanization, Ministry of Agriculture and Rural Affairs, Nanjing, Jiangsu / China
Tel: +86-15366092920; E-mail: yuanwensheng@caas.cn
Corresponding author: Wensheng YUAN
DOI: https://doi.org/10.35633/inmateh-78-97

Keywords: *Soybean seed, Response surface methodology, Genetic algorithm–backpropagation neural network, Discrete element method, Pneumatic seed metering device*

ABSTRACT
To improve the accuracy and stability of discrete element method (DEM) parameter calibration for soybean seeds under sowing conditions, a soybean seed DEM model was established in EDEM based on the intrinsic mechanical properties of seeds at sowing-stage moisture content. Free-fall collision, inclined-plane sliding, and inclined-plane rolling tests were conducted to determine the initial ranges of the seed–material contact parameters. The experimentally measured angle of repose (23.02°) was selected as the calibration index because it reflects the bulk flowability and inter-particle interaction behavior of soybean seeds. A steepest ascent test was first used to identify the sensitive inter-particle contact parameters, after which response surface methodology (RSM) and a GA-BP-GA framework were employed for optimization. The optimal parameter combination consisted of a coefficient of restitution of 0.27, a static friction coefficient of 0.23, and a rolling friction coefficient of 0.056, yielding a simulated angle of repose of 22.35° with a relative error of 2.91%, lower than that obtained by RSM alone (4.39%). Bench tests further confirmed the reliability of the calibrated model and parameters.

摘要
为提高播种工况下大豆种子离散元法（DEM）参数标定的精度与稳定性，基于播种期含水率条件下大豆种子的本征力学特性，在 EDEM 中建立了大豆种子离散元模型。通过自由落体碰撞试验、斜面滑动试验和斜面滚动试验，确定了种子–材料接触参数的初始取值范围。将试验测得的堆积角（23.02°）作为标定指标，因为其能够反映大豆种子的群体流动性和颗粒间相互作用行为。首先采用最陡爬坡试验识别敏感的颗粒间接触参数，随后结合响应面法（RSM）和 GA-BP-GA 框架进行优化。最优参数组合为恢复系数 0.27、静摩擦系数 0.23 和滚动摩擦系数 0.056，对应的仿真堆积角为 22.35°，相对误差为 2.91%，低于仅采用 RSM 时的 4.39%。台架试验进一步验证了所标定模型及参数的可靠性。

INTRODUCTION

Soybean is an important grain-and-oil crop with high nutritional and economic value *(Li, 2020)*. In recent years, the increasing demand for soybean has placed higher requirements on the efficiency and precision of mechanized sowing. However, the relatively low level of mechanized production still constrains the development of the soybean industry *(Hu et al., 2022; Ni et al., 2019)*. Although extensive studies have been conducted on pneumatic seed-metering devices *(Jia et al., 2018)*, most have focused on general-purpose designs, while relatively limited attention has been paid to the motion behavior of soybean seeds during the seed-metering process. Therefore, accurate calibration of the DEM contact parameters of soybean seeds is essential for revealing their motion characteristics during seed metering and for improving the design and performance of pneumatic soybean seed-metering devices.

With the rapid development of numerical simulation technology, the discrete element method (DEM) has become an important tool for studying the contact behavior and motion characteristics of agricultural granular materials *(Wu et al., 2024; Cundall & Strack, 1979; Maraveas et al., 2025; Yan et al., 2022)*. Existing studies have carried out DEM parameter calibration for various crop seeds, including rice *(Liu et al., 2019)*, maize *(Wang et al., 2016)*, wheat *(Liu et al., 2016)*, and mung bean *(Zhang et al., 2022)*.

However, research on DEM contact parameter calibration for soybean seeds under sowing-stage moisture conditions remains limited. Most available soybean-related parameters were obtained under harvesting *(Shu et al., 2022)*, threshing, or cleaning conditions *(Wang et al., 2023; Yu et al., 2015)*, which differ significantly from the sowing process in terms of seed moisture state and contact environment. Since the contact behavior and bulk flow characteristics of soybean seeds are highly sensitive to moisture content, these parameters cannot be directly applied to the simulation of sowing processes *(Ahmad et al., 2021; Gao et al., 2012; Tang et al., 2016)*. Therefore, it is necessary to calibrate the DEM contact parameters of soybean seeds under actual sowing-stage moisture conditions to improve the reliability of soybean seed simulation.

At present, response surface methodology (RSM) is commonly used for DEM parameter calibration because of its clear experimental design and effectiveness in factor screening and preliminary optimization. However, when the system response exhibits strong nonlinear characteristics, a single response surface model may be insufficient to accurately describe the complex relationship between contact parameters and macroscopic response indices. In contrast, intelligent optimization methods combining genetic algorithms and neural networks provide stronger nonlinear fitting and global search capability, making them more suitable for multivariable coupled problems. Therefore, in this study, RSM was first employed to determine the sensitive parameter ranges and obtain preliminary solutions, and a GA-BP-GA method was further introduced for inverse optimization to improve the accuracy, stability, and reliability of the DEM parameter calibration results *(Ding et al., 2023)*.

In this study, the physical and intrinsic mechanical properties of soybean seeds under sowing conditions were first measured, and a discrete element model of soybean seeds was then established. Free-fall collision, inclined-plane sliding, inclined-plane rolling, and angle-of-repose tests were conducted to determine the initial parameter ranges and calibrate the contact parameters. A steepest ascent design and a quadratic orthogonal rotary combination design were employed to optimize the inter-particle parameters, and the GA-BP-GA method was further introduced for inverse optimization and comparative analysis. Finally, bench experiments using a pneumatic soybean seed-metering device were carried out to validate the reliability of the developed DEM model and the calibrated parameter set.

MATERIALS AND METHODS

Soybean seeds and determination of physical and intrinsic mechanical properties

The shape and size of soybean seeds have an important influence on the seed pickup performance of pneumatic seed-metering devices. To obtain accurate geometric parameters for DEM modeling, the three principal dimensions of soybean seeds were measured in this study. A soybean cultivar commonly grown in the Huang–Huai–Hai Plain of China was selected as the test material *(Liu & Yin, 2016)*. A total of 100 soybean seeds were randomly selected for measurement. The seed length (L), width (W), and thickness (H) were measured using a digital vernier caliper with an accuracy of 0.01 mm. Based on these measurements, the equivalent diameter (d) and sphericity (φ) of soybean seeds were calculated using Eqs. (1) and (2), respectively. These parameters were used to characterize the overall size and shape of soybean seeds and to provide a basis for subsequent DEM particle model construction and simplification.

$$d = \sqrt[3]{LWH} \tag{1}$$

$$\varphi = \frac{\sqrt[3]{LWH}}{L} \times 100\% \tag{2}$$

The mass of soybean seeds was measured using an MHZ2001A electronic balance with an accuracy of 0.01 g. Each measurement was repeated ten times. Seed density was determined by the liquid displacement method. In each test, 50 soybean seeds were weighed and then placed into a 100 mL graduated cylinder containing 50 mL of distilled water. After the seeds were fully submerged and no visible air bubbles remained, the displaced liquid volume was recorded *(Yang, 2024)*. Each test was repeated ten times, and the average value was used for subsequent calculation. The seed density (ρ) was calculated as follows:

$$\rho = \frac{M}{V} \tag{3}$$

where: M is the mass of the soybean seeds (g); V is the volume of liquid displaced by the soybean seeds (cm³).

The intrinsic mechanical properties of soybean seeds mainly include Poisson's ratio, elastic modulus, and shear modulus *(Elskamp et al., 2017)*. Poisson's ratio (μ) is defined as the ratio of transverse strain to axial strain under uniaxial compression and is used to characterize the lateral deformation behavior of soybean

seeds. Uniaxial compression tests were conducted using a universal testing machine with a rated load of 5 kN and a compression platen diameter of 100 mm. Prior to testing, the relevant seed dimensions were measured using a digital vernier caliper with an accuracy of 0.01 mm, and the seeds were then placed on the testing platform. The loading speed was set to 5 mm·min^{-1}. During the test, the universal testing machine was connected to a computer for real-time acquisition of load and deformation data, and the corresponding load–deformation curves were generated automatically. After compression, the seed dimensions were measured again. The experiment was repeated five times, and the average values were used for subsequent calculation and analysis.

Poisson's ratio was calculated as follows:

$$\mu = \frac{\varepsilon'}{\varepsilon} = \frac{(b - B')/B'}{(L' - l)/L'} \tag{4}$$

where: μ is the Poisson's ratio of the seed; μ' is the transverse strain of the seed; ε is the axial strain of the seed; L' and l are the seed length before loading and at fracture, respectively; and B' and b are the seed width before loading and at fracture, respectively.

The elastic modulus was calculated as follows

$$E = \frac{0.338F(1-\mu^2)}{D^{\frac{3}{2}}}\left[K_U\left(\frac{1}{R_U}+\frac{1}{R'_U}\right)^{\frac{1}{3}} + K_L\left(\frac{1}{R_L}+\frac{1}{R'_L}\right)^{\frac{1}{3}}\right]^{\frac{3}{2}} \tag{5}$$

where: E is the elastic modulus of the soybean seed (MPa); F is the load applied to the soybean seed (N); D is the deformation of the soybean seed (mm); μ is the Poisson's ratio of the soybean seed; $R_{U,}$ R'_U and R_L, R'_L are the radii of curvature at the contact points between the upper surface of the soybean seed and the upper platen, and between the lower surface of the soybean seed and the lower base plate, respectively (mm); and K_U, K_L the curvature coefficient.

The shear modulus was calculated as follows:

$$G = \frac{E}{2(1+\mu)} \tag{6}$$

where: G is the shear modulus of the soybean seed (Pa).

Construction of the DEM particle model and selection of the contact model

The discrete element method (DEM) is a numerical approach based on Newton's laws of motion and is widely used to simulate the mechanical behavior of discrete particulate systems. Considering that soybean seeds generally exhibit an ellipsoidal shape, a multi-sphere clumping method was adopted to approximate their geometric morphology *(Zhang et al., 2022)*. Based on the measured distributions of the three principal dimensions of soybean seeds, a three-dimensional geometric model was constructed using SolidWorks software and subsequently imported into EDEM 2023 for discrete element simulation analysis. On this basis, three simplified soybean particle models with different configurations were established, and their structural schematics are shown in Fig. 1. Taking both computational efficiency and shape fidelity into consideration, a clumped-sphere model composed of 12 spheres was adopted for the subsequent simulations as a compromise between geometric representation and computational cost.

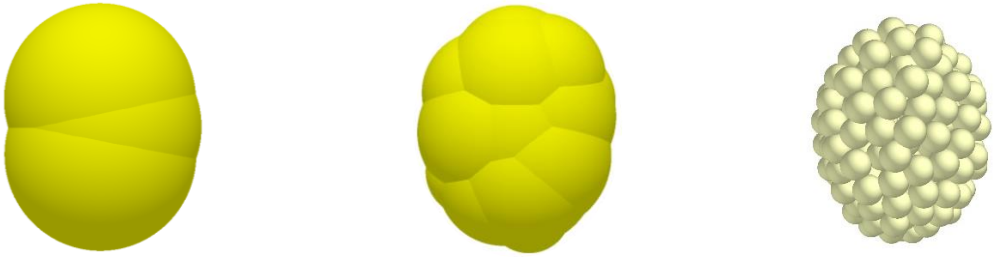

(a) Three-sphere clumped model; (b) Twelve-sphere clumped model; (c) Multi-sphere clumped model

Fig. 1 – Discrete element models of soybean seeds

During the discrete element simulations, contact interactions occurred not only among particles but also between particles and the material surfaces of the seed-metering device. To more accurately describe the force state and motion characteristics of soybean seeds within the seed-metering system, Somos 8000

resin and stainless steel were selected as representative contact materials, and their main physical properties are listed in Table 1 *(Wang et al., 2022)*.

Considering the relatively smooth surfaces of soybean seeds and the contact materials, the Hertz-Mindlin (no-slip) contact model was adopted in the EDEM simulations to calculate both particle-particle and particle-material contact behaviors, thereby providing a closer representation of the actual contact mechanics.

Table 1

Simulation parameters of contact materials

Material	Parameter	Value
Stainless steel	Density (kg·m⁻³)	7980
	Poisson's ratio	0.30
	Shear modulus / Pa	7.9×10^{10}
Somos 8000 resin	Density (kg·m⁻³)	1454.7
	Poisson's ratio	0.35
	Shear modulus / Pa	1.2×10^{8}

Experimental methods for determining seed-material contact parameters

Coefficient of restitution test

The normal coefficient of restitution between soybean seeds and material surfaces was determined using a free-fall collision test. During the test, a single soybean seed was released from a height of H = 150 mm above the material plate and allowed to fall freely under gravity. After impacting the material surface, the seed rebounded upward. The entire process was recorded using a high-speed camera, and the maximum rebound height (h) was measured. A schematic illustration of the experimental setup is shown in Fig. 2. The coefficient of restitution (e) is defined as the ratio of the normal separation velocity to the normal approach velocity at the contact point during collision. According to the kinematic relationship of free fall and rebound, the coefficient of restitution can be calculated as follows:

$$e = \frac{v_1}{v_0} = \frac{\sqrt{2gh}}{\sqrt{2gH}} = \sqrt{\frac{h}{H}} \tag{7}$$

where: e is the coefficient of restitution, v_1 is the normal separation velocity after collision, v_0 is the normal approach velocity before collision, h is the maximum rebound height, H is the initial drop height, and g is the gravitational acceleration.

Each physical experiment was repeated ten times for both Somos 8000 resin and stainless steel surfaces. To determine the effective coefficient of restitution used in the DEM simulations, numerical tests were further conducted following the same collision procedure. In the simulations, all contact parameters other than the coefficient of restitution were set to zero. The simulation coefficient of restitution (e_x) was taken as the test factor, and the rebound height was used as the evaluation index. The value of $e_x$was varied from 0.1 to 0.8 with an interval of 0.1. Each simulation condition was repeated ten times, and the average value was used for subsequent analysis.

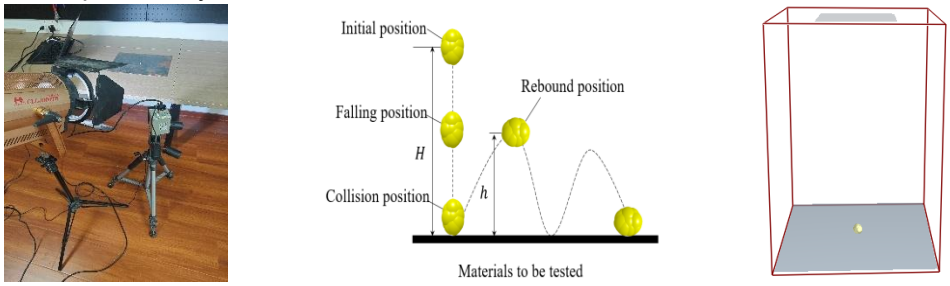

Fig. 2 – Experimental setup for calibration of the coefficient of restitution

Static friction coefficient test

The static friction coefficient between soybean seeds and material surfaces was determined using the inclined-plane sliding method *(Lima et al., 2021)*. The experimental setup is shown in Fig. 3. When a soybean seed remains at rest on an inclined plane with an inclination angle of α, the gravitational force can be resolved into a component parallel to the plane and a normal component perpendicular to the plane. As the inclination angle gradually increases, the tangential component of gravity acting along the plane also increases.

When this component reaches the maximum static friction force, the seed begins to slide relative to the inclined surface. The static friction coefficient can then be calculated as follows:

$$\mu_f = \frac{F_f}{F_N} = \frac{mg\sin\alpha}{mg\cos\alpha} = \tan\alpha \tag{8}$$

where: μ_f is the static friction coefficient, F_f is the static friction force, F_N is the normal force, m is the seed mass, g is the gravitational acceleration, and α is the critical inclination angle at which sliding occurs.

During the experiment, soybean seeds were placed on an inclined plane rigidly connected to the target contact material, and the inclination angle was increased gradually at a constant rate. When the initial sliding of the soybean seed occurred, the corresponding inclination angle was recorded. For each contact material, the test was repeated ten times, and the average value was used for subsequent analysis. To determine the effective static friction coefficient used in the DEM simulations, numerical tests were further carried out following the same sliding procedure. In the simulations, the static friction coefficient was taken as the test factor, while the critical inclination angle was used as the evaluation index. The simulation results were used for subsequent fitting and parameter calibration.

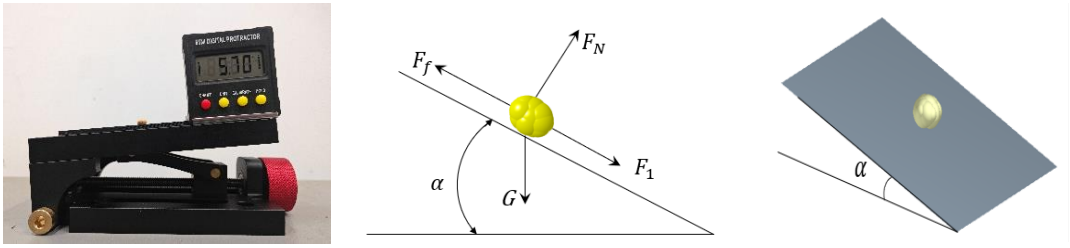

Fig. 3 – Experimental setup for static friction coefficient calibration

Rolling friction coefficient test

The rolling friction coefficient between soybean seeds and material surfaces was determined using the inclined-plane rolling method, as shown in Fig. 4 *(Zhang et al., 2022)*. In the test, the inclined plane was fixed at an inclination angle of β, and a single soybean seed was released from rest at the upper end of the plane. The seed rolled down the inclined plane for a distance S and then entered a horizontal surface, where its kinetic energy gradually dissipated due to rolling friction. The seed continued to roll on the horizontal surface for a distance L before coming to rest.

$$mgsin\beta = mg(Scos\beta + L)\mu_s \tag{9}$$

where: μ_s is the rolling friction coefficient, β is the inclination angle of the plane, S is the rolling distance on the inclined plane, and L is the rolling distance on the horizontal surface.

Because soybean seeds have an ellipsoidal shape rather than that of an ideal sphere, excessively large values of β or S may induce bouncing during rolling and thus reduce measurement accuracy, whereas excessively small values may reduce the resolution of the test. Based on preliminary trials, the inclination angle β was set to 20°, and the rolling distance S was set to 300 mm. During the experiment, a single soybean seed was released from rest at the upper end of the inclined plane, and the horizontal rolling distance L was recorded after the seed came to rest. Each test condition was repeated ten times, and the average value was used for subsequent analysis.

To determine the effective rolling friction coefficient used in the DEM simulations, numerical tests were further carried out following the same rolling procedure. In the simulations, the calibrated coefficient of restitution and static friction coefficient were predefined, while the rolling friction coefficient was taken as the test factor. The rolling friction coefficient was varied from 0.01 to 0.10 with an interval of 0.01, and the horizontal rolling distance was used as the evaluation index for subsequent fitting and parameter calibration.

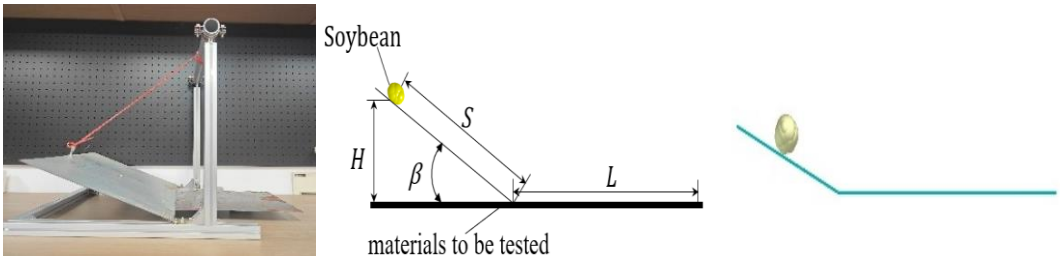

Fig. 4 – Experimental setup for rolling friction coefficient calibration

Angle-of-repose test and image-processing method

The angle of repose of soybean seeds is affected by their geometric characteristics and contact properties. In this study, the bottomless-cylinder method was used to determine the angle of repose of soybean seeds. Considering the dimensional characteristics of the seeds, a hollow cylindrical container with an outer diameter of 70 mm, an inner diameter of 66 mm, and a height of 250 mm was used. The base plate was a square flat plate with a side length of 300 mm. The experimental apparatus was fabricated from stainless steel and Somos 8000 resin, both with a thickness of 2 mm. The corresponding physical and simulation setups are shown in Fig. 5. All angle-of-repose tests were conducted at a seed moisture content of 13.79% (w.b.). During the test, the cylinder was filled with soybean seeds and then lifted vertically at a constant speed, allowing the seeds to discharge freely from the bottom opening and form a stable particle pile on the base plate. Each test was repeated ten times, and the average value was used for subsequent analysis.

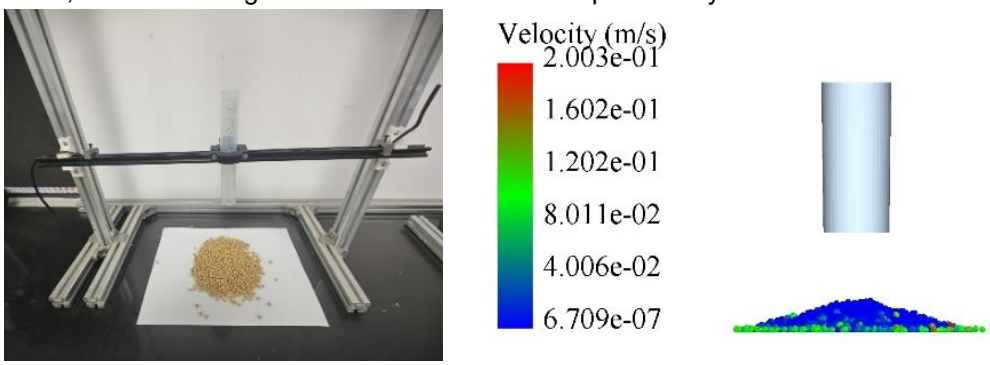

Fig. 5 – Experimental setup for the angle of repose test

After the angle-of-repose tests, images of the particle pile were processed using MATLAB, as shown in Fig. 6. First, the original images were converted to grayscale and then binarized to extract the contour of the pile. Subsequently, the edge information of the binary images was obtained, and linear fitting was performed based on the boundary points. The angle between the fitted line and the horizontal plane was taken as the measured angle of repose, denoted by (θ).

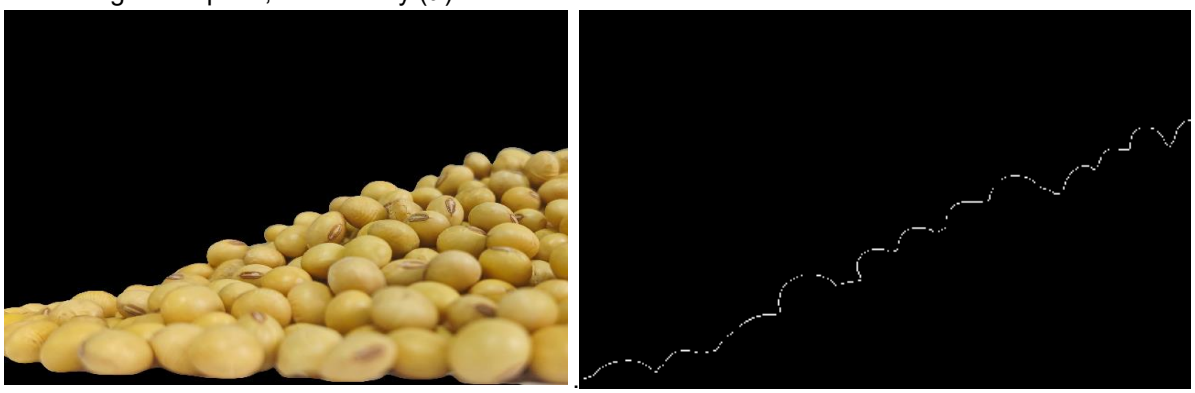

(a) grayscale and binarization *(b) edge extraction*

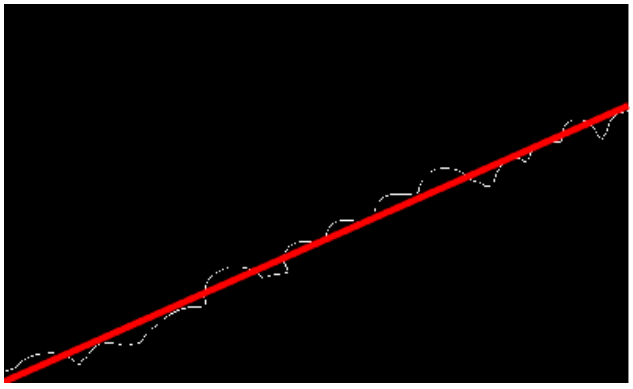

(c) linear fitting

Fig. 6 – Image processing procedure for angle of repose measurement using MATLAB

Steepest ascent experiment and RSM design

To determine appropriate ranges for the inter-particle contact parameters, a steepest-ascent experimental design was first conducted in EDEM. Based on the previously calibrated contact parameters between soybean seeds and Somos 8000 resin, the inter-particle coefficient of restitution (e), static friction coefficient (μ_f), and rolling friction coefficient (μ_r) were selected as the investigated factors. Among them, the static friction coefficient and rolling friction coefficient were considered the major factors affecting the piling behavior of soybean seeds. The experimentally measured angle of repose (θ) was used as the reference value, and the relative error between the simulated angle of repose (θ') and the measured angle of repose was used as the response variable. The relative error was calculated as follows:

$$Y = \frac{|\theta' - \theta|}{\theta} \times 100\% \quad (10)$$

where: Y is the relative error, θ is the experimentally measured angle of repose, and θ' is the simulated angle of repose.

According to published studies, the coefficient of restitution of soybean seeds generally ranges from 0.10 to 0.60, the static friction coefficient ranges from 0.10 to 0.60, and the rolling friction coefficient ranges from 0.01 to 0.17 *(Chen, 2018; Dun et al., 2022; Zhang et al., 2017)*. Based on these ranges, a three-factor, five-level steepest-ascent design was established to preliminarily identify the appropriate factor region for subsequent response surface optimization. On this basis, a three-factor, five-level quadratic orthogonal rotary combination design was further adopted for response surface methodology (RSM) analysis. The inter-particle coefficient of restitution, static friction coefficient, and rolling friction coefficient were coded as factors A, B, and C, respectively, and the relative error Y was taken as the response variable. The experimental data were analyzed using Design-Expert software to establish a regression model and determine the optimal combination of inter-particle contact parameters. The coded levels of the experimental factors are listed in Table 2.

Table 2

Factors and levels in the simulation experiments

Code	Experimental factor		
	A	***B***	***C***
-1.68179	0.20	0.20	0.042
-1	0.25	0.25	0.058
0	0.30	0.30	0.074
1	0.35	0.35	0.090
1.68179	0.40	0.40	0.106

GA-BP-GA modeling and inverse optimization method

Construction of the GA-BP model

The backpropagation (BP) neural network updates network weights and biases through an error backpropagation mechanism, enabling the model output to gradually approach the expected value. However, conventional BP networks commonly suffer from drawbacks such as slow convergence, high sensitivity to the initial weights and biases, and a tendency to become trapped in local optima *(Bai et al., 2022; Li et al., 2023)*. To improve the convergence stability and fitting accuracy of the model, a genetic algorithm (GA) was introduced to optimize the initial weights and biases of the BP network. By integrating GA with the BP neural network, a GA-BP prediction model was established to characterize the nonlinear mapping relationship between the input parameters and the response variable.

In the present study, the inter-particle coefficient of restitution, static friction coefficient, and rolling friction coefficient were taken as the input variables, and the angle of repose was taken as the output variable. The BP neural network adopted a three-layer feedforward architecture consisting of an input layer, a hidden layer, and an output layer, with 3, 7, and 1 neurons, respectively. The Bayesian regularization algorithm (trainbr) was selected as the training function to improve the generalization capability of the network under small-sample conditions. The main training parameters were set as follows: the maximum number of training epochs was 1000, the target error was 1×10^{-3}, and the learning rate was 0.01. In addition, *max_fail* was set to 200 and *min_grad* was set to 1×10^{-12}.During the GA-BP modeling process, a genetic algorithm was used to perform global optimization of the initial weights and biases of the BP network. Real-coded encoding was adopted in the GA, with a population size of 100 and a maximum of 200 generations. The selection operator was based on norm geometric selection (q = 0.09), the crossover operator used arithmetic crossover (α = 1.0),

and the mutation operator employed Gaussian mutation with a mutation probability of 0.2. Boundary clipping was applied to constrain the search space. To improve the computational efficiency of the GA evaluation process, the fitness function was defined by training the network for a limited number of rapid iterations, and the mean squared error (MSE) was used as the fitness value to screen the initial weights and biases. After the optimal individual was obtained, the corresponding weights and biases were used to initialize the BP network, and the final training was completed on the full dataset using the trainbr function. The structure of the GA-BP model is shown in Fig. 7.

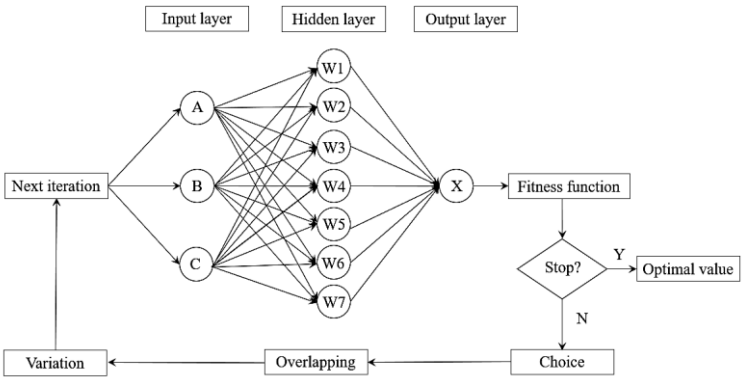

Fig. 7 – Optimal topology of the GA–BP neural network

GA-BP-GA inverse optimization procedure

Based on the established GA-BP prediction model, a genetic algorithm (GA) was further employed to perform inverse optimization of the inter-particle coefficient of restitution, static friction coefficient, and rolling friction coefficient. The experimentally measured angle of repose was taken as the target value. To ensure consistency between the optimization boundaries and the experimental dataset, the lower and upper bounds of the GA search space were defined by the minimum and maximum values of the three input variables in the training dataset. This strategy ensured that the optimization was conducted within a physically meaningful domain and avoided unreliable predictions caused by extrapolation beyond the sampled range.

In the GA-based inverse optimization process, the population size was set to 100, and the maximum number of generations was set to 100. Norm geometric selection was adopted as the selection operator with a parameter value of $q = 0.8$. The crossover operator employed arithmetic crossover with a coefficient of $\alpha = 2.0$, and the mutation probability was set to 0.2 *(Zhang et al., 2025)*. The inverse optimization results were subsequently used to determine the effective inter-particle contact parameter combination for DEM simulation.

Bench validation method

Test bench and DEM simulation setup

To verify the applicability of the calibrated contact parameters in the DEM simulation of the seed-metering process, bench-scale validation experiments were conducted using a pneumatic soybean seed-metering device. In the test device, the seed chamber was made of stainless steel, and the seed plate was fabricated from Somos 8000 resin. All validation experiments were carried out on the pneumatic seed-metering test bench at the Nanjing Research Institute for Agricultural Mechanization, Ministry of Agriculture and Rural Affairs. The structure of the test bench is shown in Fig. 8.

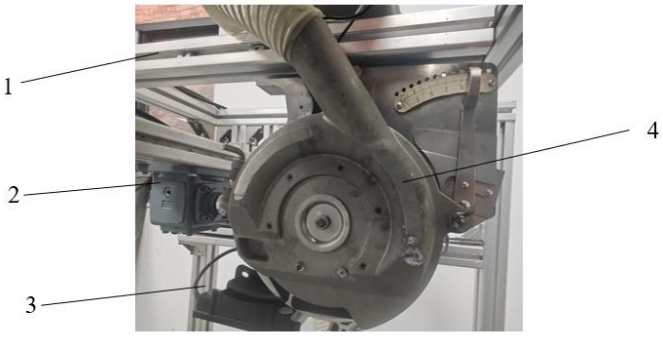

Fig. 8 – Pneumatic seed-metering test bench

1. test bench; 2. motor; 3. sensor; 4. pneumatic seed-metering device

Because the seed-metering device relies on negative pressure generated by a blower to accomplish seed pickup, the numerical simulation was conducted using an EDEM-Fluent coupled CFD-DEM approach. To improve the mesh quality of the fluid domain and enhance computational efficiency, the geometry of the seed-metering device was simplified by omitting irregular internal structures of the seed chamber while retaining the main functional components, including the seed chamber, seed plate, and air chamber. The actual and simplified models are shown in Fig. 9.

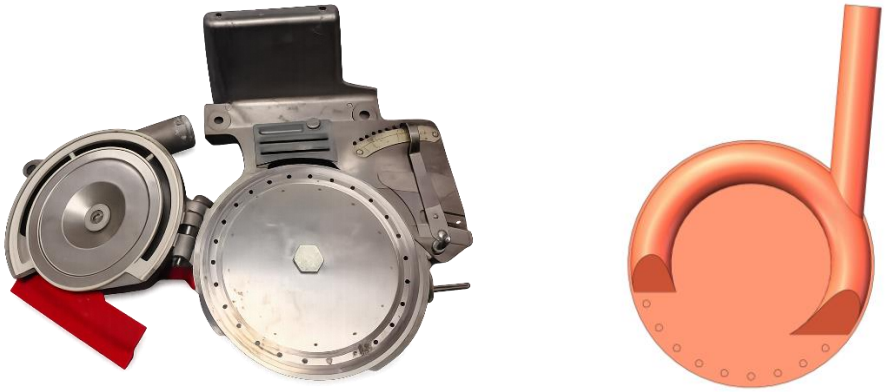

(a) actual model (b) simplified model

Fig. 9 – Seed-metering device models

The STEP-format model of the seed-metering device was exported from SolidWorks and imported into Ansys 2020 for fluid-domain mesh generation. Polyhedral meshes were used for the seed chamber, air chamber, and metering holes. In the CFD model, the negative-pressure surface of the seed chamber was defined as the inlet, and the negative-pressure surface of the air chamber was specified as the outlet. The interfaces between the seed chamber and the metering holes, as well as those between the metering holes and the suction port of the air chamber, were defined as interface boundaries. The resulting fluid-domain mesh is shown in Fig. 10.

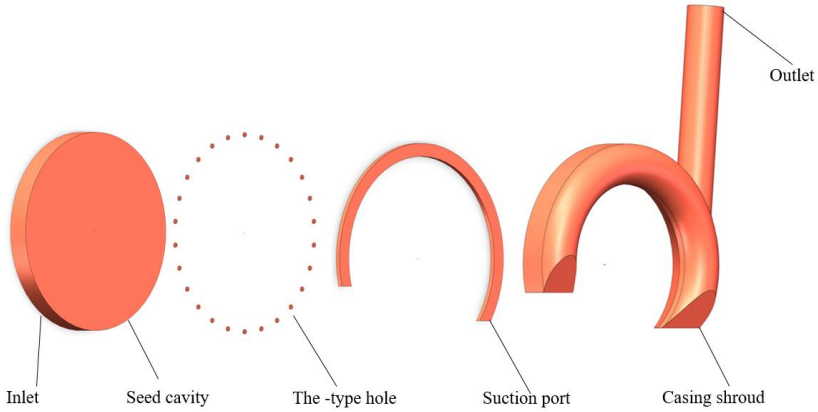

Fig. 10 – Fluid-domain mesh of the seed-metering device

Validation procedure and evaluation indices

To evaluate the accuracy of the calibrated contact parameters under operating conditions, bench tests and CFD-DEM simulations were conducted under corresponding working conditions. A single-factor experimental design was adopted, with the rotational speed of the seed plate taken as the test factor. The evaluation indices included the miss index, multiple index, and qualified index. In the bench tests, the forward speeds of the seeder were set to 8, 10, and 12 km·h^{-1}, corresponding to seed-plate rotational speeds of 49, 62, and 74 r·min^{-1}, respectively. Each operating condition was repeated three times, and the average value was used for subsequent analysis *(Shi et al., 2020; Zhou, 2021)*. For the numerical simulations, the simplified seed-metering device model was imported into EDEM 2023. The seed chamber and seed plate were assigned as stainless steel and resin, respectively. Approximately 1000 soybean seed particles were generated in the seed chamber using the previously calibrated contact parameters, and the particle state at t = 0 s was saved as the initial file. The mesh files were then imported into Fluent 2020, and the corresponding operating conditions were defined according to the seed-plate rotational speed. During the simulations, the negative pressure was set to 3, 4, and 5 kPa according to the operating conditions. Each simulation condition was repeated three times, and the average value was used for comparison with the bench-test results.

RESULTS

Physical properties of soybean seeds

Measured physical properties

The measured physical and intrinsic mechanical properties of soybean seeds are summarized in Table 3. The mean values of seed length, width, and thickness were 8.12, 7.24, and 5.98 mm, respectively, indicating that the soybean seeds exhibited a generally ellipsoidal geometry. Based on the measured triaxial dimensions, the equivalent diameter and sphericity of soybean seeds were calculated as 7.05 mm and 86.98%, respectively. The average thousand-kernel mass was 243.71 g, and the seed density determined by the liquid displacement method was 1580 kg·m^{-3}. These results provide the basic physical parameters required for subsequent DEM particle model construction and contact-parameter calibration.

Table 3

Triaxial dimensions and thousand-kernel mass of soybean seeds

Parameter	Length / mm	Width / mm	Thickness / mm	Thousand-kernel mass / g
Maximum	8.4	7.6	6.8	246.20
Minimum	7.5	6.9	5.4	241.00
Mean	8.12	7.24	5.98	243.71
Standard deviation	0.31	0.22	0.44	1.77

The intrinsic mechanical properties of soybean seeds were further determined by uniaxial compression tests. The measured Poisson's ratio, elastic modulus, and shear modulus were 0.33, 1.512×10^8Pa, and 5.6848×10^7Pa, respectively. These parameters were used as the fundamental input properties for DEM simulation of soybean seeds under sowing conditions.

DEM particle model selection

The three-sphere, twelve-sphere, and full multi-sphere models were compared in terms of geometric representation and computational efficiency. The three-sphere model provided the highest computational efficiency, but its geometric simplification was too strong to accurately capture the overall contour characteristics of soybean seeds. In contrast, the full multi-sphere model offered the best geometric detail, but it substantially increased the computational burden.

For the present EDEM–Fluent coupling case, the total physical simulation duration was preset to 6.0 s. However, the computational-time comparison among particle models was conducted for the first 1.5 s of physical simulation, which covered the complete process of seed pickup from the seed chamber, negative-pressure adsorption and transport, and seed release at the metering outlet after pressure loss. Under this condition, the elapsed computation times of the three-sphere, twelve-sphere, and full multi-sphere models were 5.8753, 8.713, and 18.111 h, respectively.

Compared with the three-sphere model, the twelve-sphere clumped model provided a more realistic approximation of the ellipsoidal geometry and contour characteristics of soybean seeds. At the same time, compared with the full multi-sphere model, the twelve-sphere model reduced the computation time by approximately 51.9% while retaining the main geometric features required for DEM simulation. Therefore, the twelve-sphere clumped model was selected for subsequent simulations as a compromise between geometric fidelity and computational efficiency.

Calibration results of seed–material contact parameters

Coefficient of restitution results

The free-fall collision tests showed that the average maximum rebound height of soybean seeds on the Somos 8000 resin plate was 17.29 mm, corresponding to an average coefficient of restitution of 0.339. In contrast, when soybean seeds collided with the stainless-steel plate, the average maximum rebound height increased to 22.93 mm, yielding an average coefficient of restitution of 0.391. These results indicate that soybean seeds exhibited a stronger rebound response on the stainless-steel surface than on the resin surface. To determine the effective coefficient of restitution for DEM simulation, the relationship between the simulated rebound height and the coefficient of restitution was fitted for the two contact materials, as shown in Fig. 11.

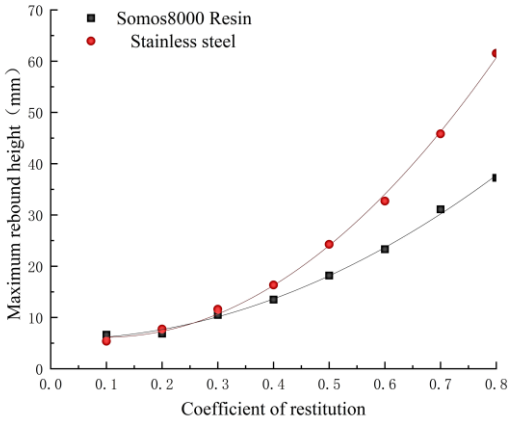

Fig. 11 – Fitted relationship between the coefficient of restitution and the maximum rebound height of soybean seeds

The fitted equations are given as follows:

$$h_1 = 5.74857 - 0.6119e_{x1} + 50.7619e_{x1}^2 (R^2 = 0.99) \quad (11)$$

$$h_2 = 7.18268 - 21.54345e_{x2} + 110.54167e_{x2}^2 (R^2 = 0.99) \quad (12)$$

where: h_1 and h_2 are the rebound heights of soybean seeds on the Somos 8000 resin and stainless-steel surfaces, respectively, and e_{x1} and e_{x2} are the corresponding effective coefficients of restitution used in the DEM simulations.

By substituting the experimentally measured average rebound heights into Eqs. (11) and (12), the effective coefficients of restitution were determined to be $e_{x1} = 0.415$ for the soybean seed–Somos 8000 resin contact pair and $e_{x2} = 0.588$ for the soybean seed–stainless steel contact pair. These values were subsequently imported into EDEM for simulation-based verification. The results showed that the relative errors between the simulated and experimentally measured rebound heights were within an acceptable range, indicating that the calibrated coefficients of restitution can reasonably characterize the collision behavior between soybean seeds and the contact materials.

Static friction coefficient results

The inclined-plane sliding tests showed that the mean critical inclination angles of soybean seeds on the Somos 8000 resin plate and the stainless-steel plate were 14.80° and 15.78°, respectively, corresponding to directly measured static friction coefficients of 0.264 and 0.282. These results indicate that the soybean seed–stainless steel contact pair exhibited slightly greater resistance to sliding than the soybean seed–Somos 8000 resin contact pair under the present test conditions. To determine the effective static friction coefficients for DEM simulation, the relationship between the simulated critical inclination angle and the static friction coefficient was fitted for the two contact materials, as shown in Fig. 12.

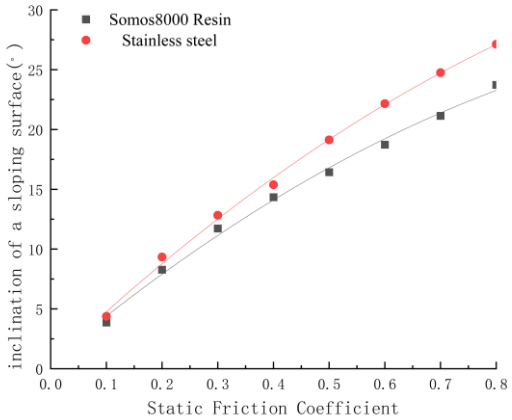

Fig. 12 – Fitted curves between the static friction coefficient and the inclination angle of the inclined plane

The fitted equations are given as follows:

$$\alpha_1 = 0.62214 + 3.1119\mu_{f1} - 13.5\mu_{f1}^2 (R^2 = 0.99) \quad (13)$$

$$\alpha_2 = 0.48446 + 44.18155\mu_{f2} - 13.6369\mu_{f2}^2 (R^2 = 0.99) \quad (14)$$

By substituting the experimentally measured critical inclination angles into Eqs. (13) and (14), the effective static friction coefficients used in the DEM simulations were determined to be $\mu_{f1} = 0.365$ for the soybean seed–Somos 8000 resin contact pair and $\mu_{f2} = 0.461$ for the soybean seed–stainless steel contact pair. These coefficients were subsequently imported into EDEM for simulation-based verification. The simulated critical inclination angles agreed well with the experimental measurements, and the deviations were within an acceptable range, indicating that the calibrated static friction coefficients can reasonably characterize the sliding behavior of soybean seeds on the two contact materials.

The DEM-calibrated static friction coefficients were higher than the directly measured values obtained from the single-seed inclined-plane tests. This difference is mainly because the inclined-plane test reflects the onset of sliding between a single soybean seed and the material surface, whereas the DEM-calibrated values are effective parameters identified from the macroscopic angle-of-repose response of a particle assembly. In addition, the soybean seed in the DEM simulation was represented by a simplified clumped-sphere model, and the contact behavior was described using an idealized Hertz-Mindlin (no-slip) model. Therefore, the calibrated static friction coefficients also compensated, to some extent, for the effects of surface roughness, particle shape irregularity, and inter-particle interaction mechanisms that were not explicitly represented in the simplified DEM model.

Rolling friction coefficient results

The inclined-plane rolling tests were conducted with an inclination angle of $\beta = 20°$and an inclined-plane rolling distance of $S = 300$ mm. Based on the results of multiple preliminary tests, the rolling distance $S$was set to 300 mm as a compromise between rolling stability and measurement sensitivity: a shorter inclined-plane distance was not sufficient to generate a clear difference in the subsequent horizontal rolling distance, whereas a longer distance tended to induce bouncing and increase the uncertainty of the measurement. Under these test conditions, the mean horizontal rolling distances of soybean seeds on the Somos 8000 resin plate and the stainless-steel plate were 182.9 and 206.1 mm, respectively. Based on the rolling test results, the directly calculated rolling friction coefficients were 0.035 for the soybean seed–Somos 8000 resin contact pair and 0.036 for the soybean seed–stainless steel contact pair. These results indicate that soybean seeds rolled farther on the stainless-steel surface than on the resin surface under the same test conditions. To determine the effective rolling friction coefficients for DEM simulation, the relationship between the simulated horizontal rolling distance and the rolling friction coefficient was fitted for the two contact materials, as shown in Fig. 13.

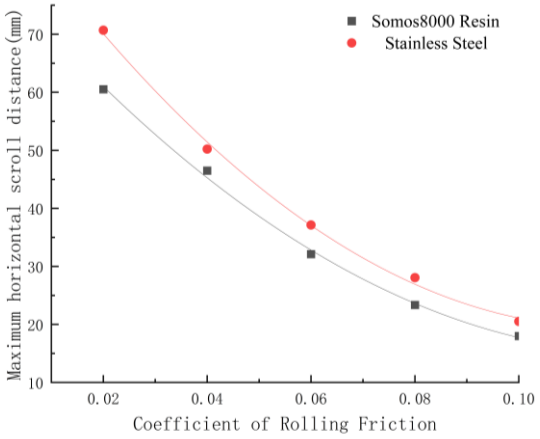

Fig. 13 – Fitted curves between the rolling friction coefficient and the horizontal rolling distance

The fitted equations are given as follows

$$L_1 = 80.038 - 1033\mu_{S1} + 4100\mu_{S1}^2 (R^2 = 0.99) \quad (15)$$

$$L_2 = 93.038 - 1253.64\mu_{S2} + 5342.85714\mu_{S2}^2 (R^2 = 0.99) \quad (16)$$

where: μ_{s1} and μ_{s2} are the rolling friction coefficients between soybean seeds and Somos 8000 resin and stainless steel, respectively; L_1 and L_2 are the horizontal rolling distances of soybean seeds on Somos 8000 resin and stainless steel, respectively.

By substituting the experimentally measured average horizontal rolling distances into Eqs. (15) and (16), the effective rolling friction coefficients used in the DEM simulations were determined to be $\mu_{s1} = 0.039$ for the soybean seed–Somos 8000 resin contact pair and $\mu_{s2} = 0.028$ for the soybean seed–stainless steel contact pair. These values were subsequently imported into EDEM for simulation-based validation. The results showed that the relative errors between the simulated and experimentally measured horizontal rolling distances were within an acceptable range, indicating that the calibrated rolling friction coefficients can reasonably characterize the rolling behavior of soybean seeds on the two contact materials. The calibrated effective rolling friction coefficients differed slightly from the directly calculated values. This difference is mainly attributed to the fact that soybean seeds are not ideal spheres but irregular ellipsoidal particles, whereas the theoretical calculation was derived under an idealized rolling assumption. Therefore, the DEM-calibrated values are more suitable as effective input parameters for subsequent numerical simulations of soybean seed motion.

Calibration results based on the angle of repose

At a seed moisture content of 13.79% (w.b.), soybean seeds formed a relatively stable particle pile in the angle-of-repose experiments, and the average measured angle of repose was 23.02°. This value was used as the target response for the subsequent calibration and optimization of the inter-particle contact parameters. The measured angle of repose reflects the combined effects of seed shape, size, moisture condition, and inter-particle contact behavior during pile formation. Therefore, it can be used as an effective macroscopic response index for inverse calibration of DEM contact parameters. In the subsequent optimization process, the relative error between the experimentally measured angle of repose and the simulated angle of repose was taken as the response variable to evaluate the accuracy of the calibrated parameter combinations.

Optimization results of the RSM model

The results of the steepest-ascent experiment are presented in Table 4. Among the six parameter combinations, the third combination yielded the smallest relative error between the simulated and experimentally measured angles of repose, with a value of 4.04%. Therefore, the second, third, and fourth combinations were selected as the reference points for the subsequent response surface optimization. These results indicate that the suitable parameter region for further optimization was located near the intermediate levels of the three investigated factors.

Table 4

Design and results of the steepest-ascent experiment

Serial number	Experimental factors			Experimental results	
	e	μ_f	μ_s	*θ′/ (°)*	*σ/ (%)*
1	0.10	0.10	0.010	12.32	46.48
2	0.20	0.20	0.042	16.38	28.84
3	0.30	0.30	0.074	22.09	4.04
4	0.40	0.40	0.106	25.95	12.73
5	0.50	0.50	0.138	29.15	29.15
6	0.60	0.60	0.170	34.55	50.09

The experimental design matrix and corresponding response values of the three-factor, five-level quadratic orthogonal rotary combination experiment are listed in Table 5. Based on these simulation results, an analysis of variance (ANOVA) was performed, and the results are presented in Table 6. The regression model was highly significant ($P = 0.0002$), whereas the lack-of-fit term was not significant ($P = 0.3467$), indicating that the established response surface model had good fitting accuracy and reliability. Among the investigated factors, the inter-particle static friction coefficient (B) and rolling friction coefficient (C) had highly significant effects on the response variable, while the effect of the inter-particle coefficient of restitution (A) was not significant. In addition, the interaction terms AC and BC, as well as the quadratic terms A^2 and B^2, were significant, indicating that the angle-of-repose error was influenced not only by the individual factors but also by their nonlinear coupling effects.

Table 5

Experimental design and results

No	Experimental factor			Y/%
	A	B	C	
1	-1	-1	-1	23.54
2	1	-1	-1	15.94
3	-1	1	-1	11.43
4	1	1	-1	12.81
5	-1	-1	1	7.26
6	1	-1	1	11.99
7	-1	1	1	7.69
8	1	1	1	11.6
9	-1.68179	0	0	14.29
10	1.68179	0	0	11.08
11	0	-1.68179	0	19.46
12	0	1.68179	0	12.16
13	0	0	-1.68179	15.51
14	0	0	1.68179	8.69
15	0	0	0	10.82
16	0	0	0	9.38
17	0	0	0	7.08
18	0	0	0	10.69
19	0	0	0	8.78
20	0	0	0	9.51
21	0	0	0	6.08
22	0	0	0	5.34
23	0	0	0	7.52

The relatively weak effect of the coefficient of restitution on the angle-of-repose response can be attributed to the ellipsoidal and irregular shape of soybean seeds. During pile formation, strong inter-particle energy dissipation occurs, which causes the rebound kinetic energy to attenuate rapidly within the particle assembly. As a result, the contribution of the coefficient of restitution to the macroscopic piling behavior becomes less pronounced than those of the static and rolling friction coefficients. In addition, because a layer of soybean seeds was pre-filled at the bottom of the cylinder before the angle-of-repose test, the effect of the base material on particle rebound was further weakened, which also reduced the sensitivity of the response to the restitution coefficient

Table 6

Analysis of variance for the relative error of the angle of repose

Source	Degrees of freedom	Mean square	*F*-value	*P*-value
Model	9	39.68	9.22	0.0002**
A-A	1	0.6496	0.1510	0.7039
B-B	1	55.28	12.85	0.0033**
C-C	1	98.35	22.86	0.0004**
AB	1	8.32	1.93	0.1876
AC	1	27.60	6.42	0.0250*
BC	1	29.18	6.78	0.0218*
A^2	1	27.28	6.34	0.0257*
B^2	1	92.68	21.54	0.0005**
C^2	1	19.35	4.50	0.0538
Residual	13	4.30		
Lack of Fit	5	5.05	1.32	0.3467
Pure Error	8	3.84		
Cor Total	22			

where: * indicates a significant effect ($0.01 < P < 0.05$), and ** indicates a highly significant effect ($P < 0.01$).

Regression fitting was performed using Design-Expert software, and the resulting regression equation is expressed as follows:

$$Y = 8.38 - 0.2181A - 2.01B - 2.68C + 1.02AB + 1.86AC + 1.91BC + 1.31A^2 + 2.42B^2 + 1.10C^2 \quad (17)$$

The pairwise interaction effects of the three factors on the response variable are shown in Fig. 14. When the rolling friction coefficient was held constant, the response exhibited a pronounced quadratic variation with changes in the coefficient of restitution and static friction coefficient, indicating an evident interaction effect between these two factors. When the static friction coefficient was fixed, the response increased overall with increasing coefficient of restitution and rolling friction coefficient, suggesting a synergistic effect between the two variables. When the coefficient of restitution was held constant, the response varied nonlinearly with the static and rolling friction coefficients, and the elliptical contour distribution further confirmed the significant interaction between these two friction-related parameters.

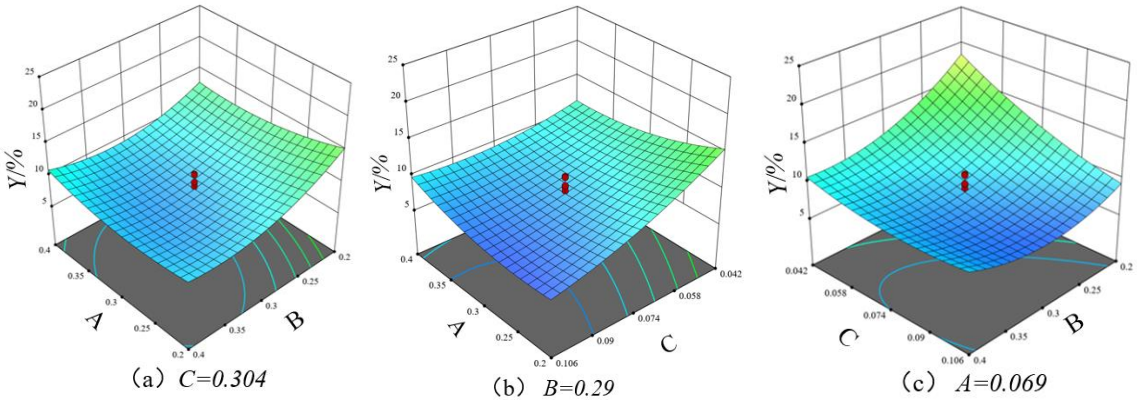

Fig. 14 – Response surface and contour plots showing the interaction effects of contact parameters on the angle of repose

Based on the regression model, the inter-particle contact parameters were optimized by minimizing the relative error between the experimentally measured angle of repose and the simulated angle of repose. The optimization objective and constraints are expressed as follows:

$$\begin{cases} minY(A,B,C) \\ s.t. \begin{cases} -1.68179 \le A \le 1.68179 \\ -1.68179 \le B \le 1.68179 \\ -1.68179 \le C \le 1.68179 \end{cases} \end{cases} \quad (18)$$

The optimal inter-particle contact parameters obtained by RSM were a coefficient of restitution of 0.304, a static friction coefficient of 0.29, and a rolling friction coefficient of 0.069. These parameters were subsequently imported into EDEM for simulation verification. The results showed that the relative error between the simulated and experimentally measured angles of repose was 4.39%, indicating that the optimized parameter combination can effectively characterize the actual piling behavior of soybean seeds and can be used as a preliminary calibrated parameter set for subsequent DEM simulations.

Inverse optimization results of the GA-BP-GA model

The performance curve of the GA-BP neural network is shown in Fig. 15.

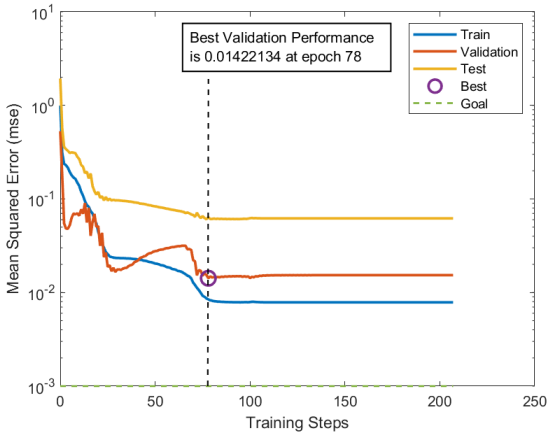

Fig. 15 – Performance curve of the GA–BP neural network

During the second training stage, the model achieved its best validation performance with a mean squared error (MSE) of 0.01422134, indicating that the proposed GA-BP model had good convergence behavior and fitting accuracy for the available experimental data.

This result suggests that the model was able to capture the nonlinear relationship between the inter-particle contact parameters and the angle of repose with satisfactory stability.

The predictive capability of the optimized GA-BP neural network was further evaluated by regression analysis, as shown in Fig. 16. The correlation coefficients (R) for the training, validation, and test datasets were 0.98268, 0.88215, and 0.97695, respectively, and the overall correlation coefficient reached 0.95934. These results indicate a strong agreement between the predicted and measured values, confirming that the established GA-BP model had good fitting and predictive performance and was suitable for subsequent inverse optimization of the contact parameters.

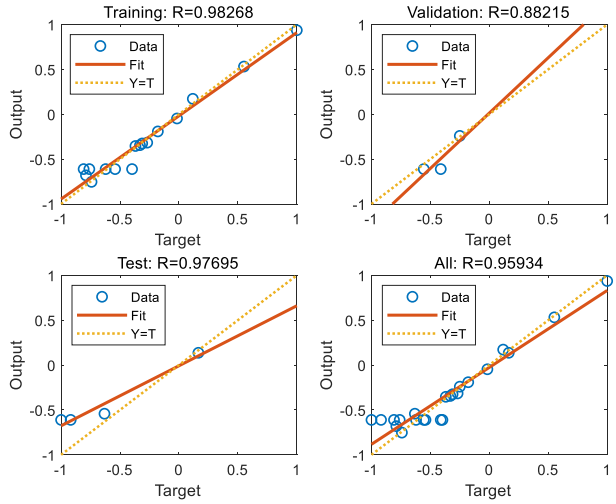

Fig. 16 – Regression analysis of the GA–BP neural network model

The variation of the fitness value during the GA-based inverse optimization process is shown in Fig. 17. As the number of iterations increased, the fitness value decreased rapidly in the initial stage and then gradually converged to a stable level, indicating that the genetic algorithm exhibited good global search capability and convergence behavior within the parameter search space. The smooth overall trend of the fitness curve further demonstrates the stability and reliability of the inverse optimization process.

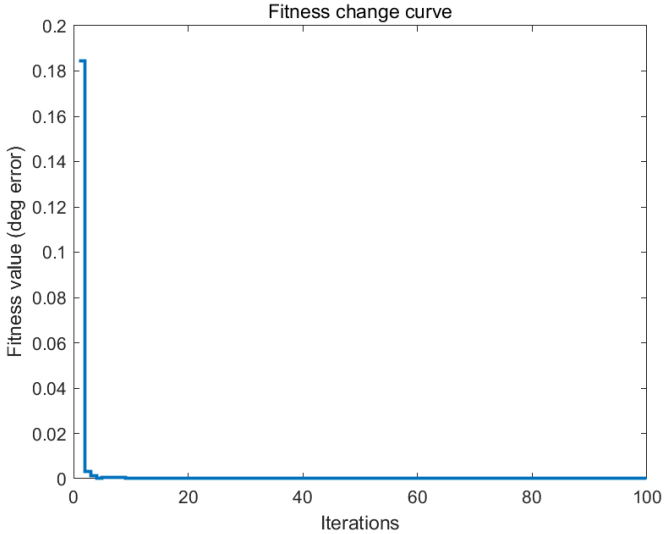

Fig. 17 – Variation curve of the fitness value during the GA optimization process

Based on the GA-BP-GA inverse optimization results, the optimal inter-particle contact parameters of soybean seeds were determined to be a coefficient of restitution of 0.27, a static friction coefficient of 0.23, and a rolling friction coefficient of 0.056. Under this parameter combination, the simulated angle of repose was 22.35°, corresponding to a relative error of 2.91% compared with the experimentally measured angle of repose. Compared with the RSM-based optimized result, whose relative error was 4.39%, the GA-BP-GA method further improved the calibration accuracy. These results indicate that the GA-BP-GA framework has better capability than RSM alone in characterizing the nonlinear mapping relationship between DEM contact parameters and the macroscopic piling behavior of soybean seeds.

Bench validation results

Representative simulation snapshots during the seed-metering process are shown in Fig. 18. At 0.1 s, only a small number of soybean seeds were adsorbed by the metering holes, and the coupled interaction forces between the particles and the seed-metering device were relatively low, mainly appearing in blue and light green regions. At this stage, all three metering holes achieved single-seed filling without obvious missed or multiple adsorption, indicating a stable seed pickup state. When the simulation progressed to 0.5 s, the number of adsorbed seeds gradually increased, and the coupled forces of some particles increased slightly; however, the overall seed-metering process remained in a stable holding stage.

At 1.0 s, missed adsorption began to occur after approximately 0.6 s. By 0.98 s, some seeds detached after leaving the negative-pressure region because the coupled interaction force was insufficient to maintain stable adsorption. At this stage, pronounced differences in the force distribution appeared among particles near the edges of the metering holes. When the simulation further advanced to 1.5 s, multiple-seed adsorption occurred at the metering holes, and several particles accumulated near the holes. Some particles exhibited significantly increased coupled interaction forces, indicating that the adsorption state had transitioned from stable adsorption to an over-adsorption condition. These results reveal the dynamic evolution of seed filling, seed holding, missed pickup, and multiple adsorption during the seed-metering process.

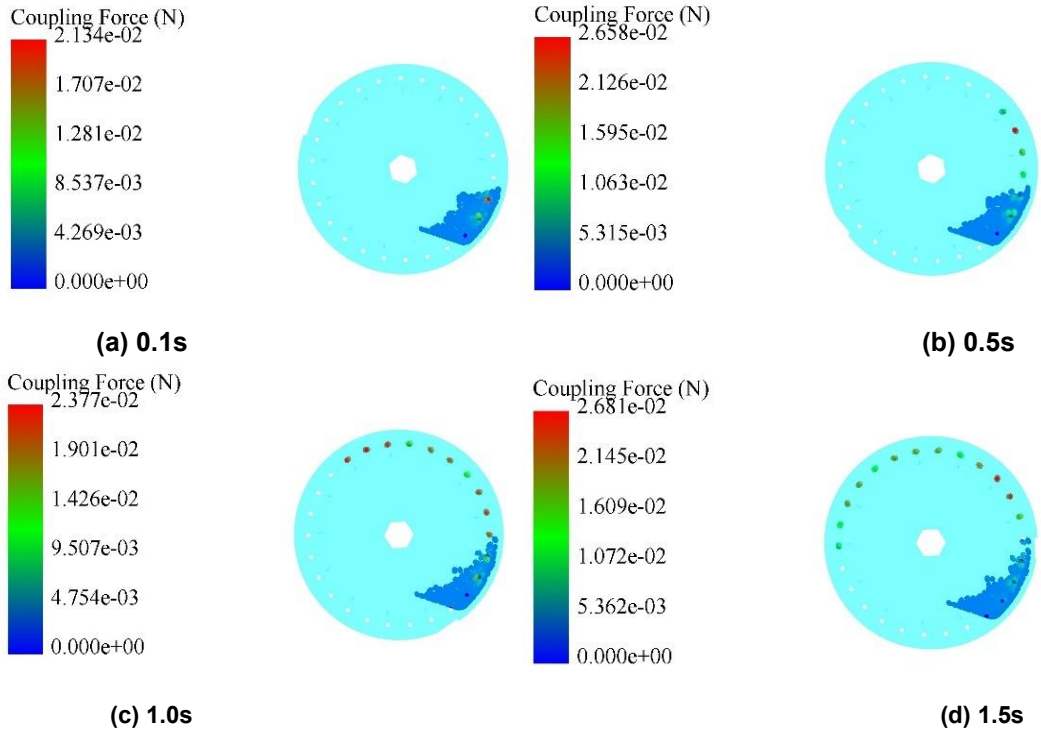

Fig. 18 – Simulation snapshots during the seed-metering process

The quantitative comparison between the bench-test results and the CFD–DEM simulation results is presented in Table 7. As the seed-plate rotational speed increased from 49 to 74 r·min^{-1}, both the miss index and the multiple index showed an overall increasing trend in the bench and simulation tests, whereas the qualified index decreased gradually. Specifically, in the bench tests, the qualified index decreased from 95.33% at 49 r·min^{-1} to 86.67% at 74 r·min^{-1}, while the corresponding simulated values decreased from 96.00% to 90.00%. These results indicate that increasing seed-plate rotational speed reduced the seed-metering performance of the pneumatic soybean seed-metering device under the tested operating conditions. A comparison under different rotational speeds showed that the average relative error of the qualified index between the simulation and bench-test results was 2.00%, with a maximum relative error of 3.84%. All errors were controlled within 5%, indicating that the established DEM model can reasonably characterize the sowing performance of the pneumatic soybean seed-metering device. Overall, the performance indices obtained from the bench tests were slightly lower than those predicted by the simulations. This discrepancy can be attributed to the fact that the simulations were conducted under relatively idealized conditions, whereas the bench tests were affected by machine vibration, model simplification, seed collisions within the seed chamber, and fluctuations in negative pressure.

Table 7

Comparison of bench test and simulation results

Test Category	Rotational speed (r/min)	Multiple index (%)	Miss index (%)	Qualification index (%)
Bench test	49	3.00	1.67	95.33
	62	4.67	3.33	91.33
	74	6.33	7.00	86.67
Simulation test	49	2.33	1.67	96.00
	62	4.33	3.00	92.67
	74	5.67	6.33	90.00

Moreover, under both low-speed and high-speed operating conditions, fluctuations in missed and multiple seeding events were more pronounced, which may have increased the dispersion of the relative errors of individual indices. Therefore, the qualified index, as a comprehensive performance metric, was selected as the primary criterion for evaluating the consistency between the simulation and bench-test results. Overall, the validation results demonstrate that the DEM model established using the calibrated contact parameters can reliably reproduce the actual motion behavior and seed-metering characteristics of soybean seeds in a pneumatic seed-metering device, thereby providing a sound basis for subsequent structural optimization and performance prediction.

CONCLUSIONS

(1) The physical and intrinsic mechanical properties of soybean seeds under sowing conditions were determined, and a DEM particle model of soybean seeds was established. Based on the measured geometric characteristics, three simplified particle models were compared, and the twelve-sphere clumped model was selected for subsequent simulations as a compromise between geometric fidelity and computational efficiency. In addition, the contact parameters between soybean seeds and the representative materials of the seed-metering device were calibrated through physical tests combined with DEM-based calibration.

(2) Using the experimentally measured angle of repose as the calibration index, the inter-particle contact parameters of soybean seeds were optimized through a steepest ascent experiment, response surface methodology (RSM), and a GA-BP-GA framework. The RSM-based optimum parameter combination yielded a relative error of 4.39% between the simulated and experimentally measured angles of repose, whereas the GA-BP-GA method further reduced the relative error to 2.91%. These results indicate that the GA-BP-GA framework outperformed RSM alone in capturing the nonlinear relationship between microscopic contact parameters and macroscopic bulk behavior.

(3) Bench validation tests of a pneumatic soybean seed-metering device showed that the average relative error of the qualified index between simulation and experiment was 2.00%, with a maximum of 3.84%. All relative errors were controlled within 5%, indicating that the calibrated DEM model can reliably characterize the seed-metering performance of soybean seeds under sowing conditions. The proposed calibration framework can therefore provide a useful reference for the DEM-based simulation, parameter calibration, and performance optimization of pneumatic seed-metering devices, and may also be extended to similar seed particles under comparable operating conditions.

ACKNOWLEDGEMENT

This research was supported by the National Key Research and Development Program of China (Grant No. 2021YFD2000503), the China Agriculture Research System for Soybean (CARS-04), and the Agricultural Science and Technology Innovation Program (Grant No. CAAS-ZDRW202413).

REFERENCES

[1] Ahmad, R. K., Dangora, N. D., & Ahmad, H. K. (2021). Effect of moisture content on soybean engineering properties: comparative study of varieties（含水率对大豆工程特性的影响：不同品种比较）. *Agricultural Engineering International: CIGR Journal*, 23(1), 225–234.

[2] Bai, Y., Xie, W., Zhao, M., Zhou, K., Fan, R., Guan, T., Sun, H., & Dai, C. (2022). Contact parameter calibration of starch discrete element method based on BP neural network of MATLAB（基于 MATLAB 的 BP 神经网络法标定淀粉离散元接触参数）. *Chinese Pharmaceutical Journal, 57*(15), 1268–1277. https://doi.org/10.11669/cpj.2022.15.007

[3] Chen, Y. L. (2018). *Research on air-suction mechanical compound high-speed precision soybean seed metering device*（*气吸机械复合式大豆高速精密排种器的研究*）(Doctoral dissertation, Jilin University).

https://kns.cnki.net/KCMS/detail/detail.aspx?dbcode=CDFD&dbname=CDFDLAST2018&filename=1018073305.nh

[4] Cundall, P. A., & Strack, O. D. L. (1979). A discrete numerical model for granular assemblies（颗粒集合体的离散数值模型）. *Géotechnique, 29*(1), 47–65. https://doi.org/10.1680/geot.1979.29.1.47

[5] Ding, X. T., Li, K., Hao, W., Yang, Q. C., Yan, F. X., & Cui, Y. J. (2023). Calibration of camellia seed simulation parameters based on RSM and GA-BP-GA optimization（基于响应面法与遗传算法优化的BP 神经网络标定油茶籽仿真参数）. *Transactions of the Chinese Society of Agricultural Machinery, 54*(2), 139–150. https://doi.org/10.6041/j.issn.1000-1298.2023.02.013

[6] Dun, G. Q., Mao, N., Liu, W. H., Wu, X. P., Zhou, C., & Ji, W. Y. (2022). Design and test of four-bar translational soybean plot breeding seed metering device（四杆平移式大豆小区育种排种器设计与试验）. *Transactions of the Chinese Society of Agricultural Machinery, 53*(4), 70–78. https://doi.org/10.6041/j.issn.1000-1298.2022.04.007

[7] Elskamp, F., Kruggel-Emden, H., Hennig, M., & Teipel, U. (2017). A strategy to determine DEM parameters for spherical and non-spherical particles（一种确定球形与非球形颗粒离散元参数的方法）. *Granular Matter, 19*(3), Article 46. https://doi.org/10.1007/s10035-017-0710-0

[8] Gao, L. X., Jiao, W. P., Yang, D. X., Shao, Z. G., Zhao, X. G., & Liu, D. J. (2012). Effect of moisture content on static mechanical properties of soybeans（含水率对大豆静态力学特性的影响）. *Transactions of the Chinese Society of Agricultural Engineering, 28*(15), 40–44. https://doi.org/10.3969/j.issn.1002-6819.2012.15.007

[9] Hu, P. J., Yang, S. D., & Liu, Y. (2022). Current status and development trend of soybean sowing machinery（大豆播种机械的发展现状与趋势）. *Shandong Agricultural Mechanization*, (1), 46–47. https://doi.org/10.15976/j.cnki.37-1123/s.2022.01.020

[10] Jia, H. L., Chen, Y. L., Zhao, J. L., Wang, J. X., Guo, M. Z., & Zhuang, J. (2018). Design and test of air-suction mechanical compound precision soybean seed metering device（气吸机械复合式大豆精密排种器设计与试验）. *Transactions of the Chinese Society of Agricultural Machinery, 49*(4), 75–86, 139. https://doi.org/10.6041/j.issn.1000-1298.2018.04.008

[11] Li, A. C. (2020). Research progress on main nutritional components and nutritional value of soybeans（大豆主要营养成分及营养价值研究进展）. *Modern Agricultural Science and Technology*, (23), 213–214, 218.

[12] Li, G., Ma, J., Tian, X., Zhao, C., An, S., Guo, R., Feng, B., & Zhang, J. (2023). Discrete meta-simulation of silage based on RSM and GA-BP-GA optimization parameter calibration（基于响应面法与遗传算法优化的BP 神经网络标定青贮饲料离散元仿真参数）. *Processes, 11*(9), Article 2784. https://doi.org/10.3390/pr11092784

[13] Lima, R. M., Brandao, R. J., Santos, R. L., Duarte, C. R., & Barrozo, M. A. S. (2021). Analysis of methodologies for determination of DEM input parameters（离散元输入参数的测定方法分析）. *Brazilian Journal of Chemical Engineering, 38*(2), 287–296. https://doi.org/10.1007/s43153-021-00107-4

[14] Liu, F. Y., Zhang, J., Li, B., & Chen, J. (2016). Analysis and calibration of wheat discrete element parameters based on stacking test（基于堆积试验的小麦离散元参数分析与标定）. *Transactions of the Chinese Society of Agricultural Engineering, 32*(12), 247–253. https://doi.org/10.11975/j.issn.1002-6819.2016.12.035

[15] Liu, L. J., & Yin, S. Z. (2016). Current status and development trend of summer soybean production mechanization in the Huang-Huai-Hai region（黄淮海地区夏大豆生产机械化发展现状与趋势）. *Modern Agricultural Research*, (1), 16–19.

[16] Liu, Y. P., Zhang, T., & Liu, Y. (2019). Calibration and test of discrete element contact parameters for rice grain model（稻谷颗粒模型离散元接触参数标定与试验）. *Journal of Agricultural Science and Technology, 21*(11), 70–76. https://doi.org/10.13304/j.nykjdb.2018.0730

[17] Maraveas, C., Tsigkas, N., & Bartzanas, T. (2025). Agricultural processes simulation using discrete element method: A review（基于离散元法的农业过程仿真研究综述）. *Computers and Electronics in Agriculture, 237*, 110733. https://doi.org/10.1016/j.compag.2025.110733

[18] Ni, Y. L., Jin, C. Q., Chen, M., Wang, T. E., Li, Z. F., & Yuan, W. S. (2019). Research progress on key technologies and equipment of soybean mechanized production in China（我国大豆机械化生产关键技术与装备研究进展）. *Journal of Chinese Agricultural Mechanization, 40*(12), 17–25.

https://doi.org/10.13733/j.jcam.issn.2095-5553.2019.12.04

[19] Shi, S., Liu, H., Wei, G. J., Zhou, J. L., Jian, S. C., & Zhang, R. F. (2020). Optimization and test of air-suction seed metering device with guide-assisted seed filling based on DEM-CFD（基于离散元 - 计算流体力学耦合的导种辅助充种气吸式排种器优化与试验）. *Transactions of the Chinese Society of Agricultural Machinery, 51*(5), 54–66. https://doi.org/10.6041/j.issn.1000-1298.2020.05.006

[20] Shu, C. X., Yang, J., Wan, X. Y., Yuan, J. C., Liao, Y. T., & Liao, Q. X. (2022). Calibration and test of discrete element simulation parameters for rapeseed discharge during combine harvesting（联合收获油菜排种离散元仿真参数标定与试验）. *Transactions of the Chinese Society of Agricultural Engineering, 38*(9), 34–43. https://doi.org/10.11975/j.issn.1002-6819.2022.09.004

[21] Tang, F. Y., Gu, B. C., Chen, F., & Cheng, X. D. (2016). Study on the effect of moisture content on destructive force and apparent contact elastic modulus of soybean grains（含水率对大豆籽粒破坏力及表观接触弹性模量的影响研究）. *Grain Science and Technology & Economy, 41*(4), 44–48. https://doi.org/10.16465/j.gste.cn431252ts.20160413

[22] Wang, G. W., Xia, X. M., Zhu, Q. H., Yu, H. Y., & Huang, D. Y. (2022). Design and test of air-suction high-speed precision soybean seed metering device with assisted seed filling based on DEM-CFD coupling（基于离散元 - 计算流体力学耦合的辅助充种气吸式大豆高速精密排种器设计与试验）. *Journal of Jilin University (Engineering and Technology Edition), 52*(5), 1208–1221. https://doi.org/10.13229/j.cnki.jdxbgxb20211366

[23] Wang, L., Zhang, S., Gao, Y., Cui, T., Ma, Z., & Wang, B. (2023). Investigation of maize grains penetrating holes on a novel screen based on CFD-DEM simulation（基于离散元-计算流体力学仿真的玉米籽粒穿筛特性研究）. *Powder Technology, 419*, 118332. https://doi.org/10.1016/j.powtec.2023.118332

[24] Wang, Y. X., Liang, Z. J., Zhang, D. X., Cui, T., Shi, S., Li, K. H., & Yang, L. (2016). Calibration of inter-seed contact parameters for corn seed particle model based on discrete element method（基于离散元法的玉米籽粒间接触参数标定）. *Transactions of the Chinese Society of Agricultural Engineering, 32*(22), 36–42. https://doi.org/10.11975/j.issn.1002-6819.2016.22.005

[25] Wu, M. P., Wang, X. G., & Ji, H. (2024). Current status and development trend of discrete element simulation in seed metering device design（离散元仿真在排种器设计中的应用现状与发展趋势）. *Digital Agriculture and Intelligent Agricultural Machinery*, (6), 19–22.

[26] Yan, D., Yu, J., Wang, Y., Zhou, L., Sun, K., & Tian, Y. (2022). A review of the application of discrete element method in agricultural engineering: A case study of soybean（离散元法在农业工程中的应用综述——以大豆为例）. *Processes, 10*(7), Article 1305. https://doi.org/10.3390/pr10071305

[27] Yang, F. (2024). *Design and test of automatic seed metering device for soybean plot breeding*（大豆小区育种自动化排种器设计与试验）(Master's thesis, Shandong Agricultural University). https://doi.org/10.27277/d.cnki.gsdnu.2024.001048

[28] Yu, Y., Fu, H., & Yu, J. (2015). DEM-based simulation of the corn threshing process（基于离散元法的玉米脱粒过程仿真）. *Advanced Powder Technology, 26*(5), 1400–1409. https://doi.org/10.1016/j.apt.2015.07.015

[29] Zhang, H. D., Tang, Z. X., Zhang, L. Y., Yu, Q., & Song, C. J. (2025). Discrete element simulation parameter calibration of red soil for under-forest *Panax notoginseng* planting based on GA-BP-GA optimization（基于遗传算法优化的 BP 神经网络标定林下三七种植红壤离散元仿真参数）. *Journal of Agricultural Science and Technology (Chinese & English), 27*(9), 120–130. https://doi.org/10.13304/j.nykjdb.2024.0188

[30] Zhang, S. W., Zhang, R. Y., Chen, T. Y., Fu, J., & Yuan, H. F. (2022). Calibration of discrete element simulation parameters for mung bean seeds and seeding test（绿豆种子离散元仿真参数标定与排种试验）. *Transactions of the Chinese Society of Agricultural Machinery, 53*(3), 71–79. https://doi.org/10.6041/j.issn.1000-1298.2022.03.007

[31] Zhang, T., Liu, F., Zhao, M. Q., Liu, Y. Q., Li, F. L., Ma, Q., Zhang, Y., & Zhou, P. (2017). Determination of contact physical parameters between soybean seeds and seed metering device and discrete element simulation calibration（大豆籽粒与排种器接触物理参数测定及离散元仿真标定）. *Journal of China Agricultural University, 22*(9), 86–92.

[32] Zhou, R. Y. (2021). *Design and test of air-suction high-speed precision soybean seed metering device*（气吸式大豆高速精密排种器设计与试验）(Master's thesis, Jilin University). https://doi.org/10.27162/d.cnki.gjlin.2021.005239